Mesoporous Materials

DOI: 10.1002/anie.200700689

Orientational Control of Hexagonally Packed Silica Mesochannels in Lithographically Designed Confined Nanospaces**

*Chia-Wen Wu, Tetsu Ohsuna, Tomohiro Edura, and Kazuyuki Kuroda**

Two-dimensional (2D) hexagonal mesoporous silica materials have attracted much attention because of their large surface area and uniform pore size.[1,2] The 2D hexagonal mesoporous structure (*p6mm*) generally consists of hexagonally packed mesochannels which can be used as hosts for encapsulation of functional molecules and for fabrication of metal nanowires.[3,4] Depositing these mesochannels on a substrate and controlling their orientation are of special interest in optics,[5–7] nanoreactors,[8] chemical sensing,[9] low-*k* materials,[10] and fabrication of nanowire films.[11] Methods utilizing external fields,[12–17] modified substrates,[18] and chemically designed interfaces[19] have been used to orient mesochannels on the macroscopic scale. However, these alignment techniques are designed for films with a single orientation, either parallel or perpendicular to a substrate. It is difficult to selectively engineer the orientation of mesochannels at desired positions. For the development of the next generation of optical and electronic devices, the ability to create an orientation and control its direction is required.

Our studies show that lithography-assisted alignment can be a reliable and versatile route (Figure 1). So far, the combination of top-down lithographical technologies and bottom-up self-assembly chemistry has mainly focused on creating hierarchically ordered porous structures.[20,21] Trau et al. aligned mesochannels by infiltrating a surfactant-templated silica solution into lithographically prepared microcapillaries and simultaneously applying an electric field.[16] However, since this method relies on interactions between surfactants and applied electric field, it is limited to ionic surfactants (e.g., cetyltrimethylammmonium bromide) and results in restricted pore size (ca. 2 nm). Here we present a new alignment method in which a silica precursor solution templated by a poly(ethylene oxide)$_{20}$–poly(propylene oxide)$_{70}$–poly(ethylene oxide)$_{20}$ triblock copolymer (P123) is

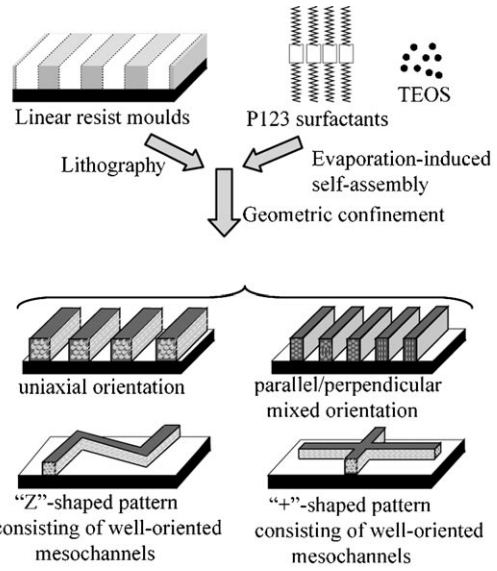

Figure 1. The fabrication of various types of mesoporous silica devices consisting of well-oriented mesochannels by a combination of lithography and evaporation-induced self-assembly.

[*] Dr. C.-W. Wu,[+] Prof. Dr. T. Ohsuna, Prof. Dr. K. Kuroda
Kagami Memorial Laboratory for Materials Science and Technology
Waseda University
Nishiwaseda 2-8-26, Shinjuku-ku, Tokyo 169-0051 (Japan)
and
CREST
Japan Science and Technology Agency (JST)
Honcho 4-1-8, Kawaguchi-shi, Saitama 332-0012 (Japan)
Fax: (+81) 3-5286-3787
E-mail: kevinwu@iastate.edu
Prof. Dr. K. Kuroda
Department of Applied Chemistry
Faculty of Science and Engineering
Waseda University
Ohkubo 3-4-1, Shinjuku-ku, Tokyo 169-8555 (Japan)
and
Consolidated Research Institute for Advanced Science and Medical Care
Waseda University
Shinjuku-ku, Tokyo 162-0041 (Japan)
E-mail: kuroda@waseda.jp
Dr. T. Edura
Nanotechnology Research Laboratory, Waseda University
513 Wasedatsurumaki-cho, Shinjuku-ku, Tokyo 162-0041 (Japan)
[+] Present address:
Department of Chemistry
Iowa State University
Ames, IA 50010 (USA)

[**] The authors thank Dr. H. Miyata (Canon Inc.) for advice and Prof. Y. Honda (Consolidated Research Institute for Advanced Science and Medical Care, Waseda University) for help with electron-beam lithography and HRSEM. This work is supported in part by the 21st Century COE Program "Practical Nano-Chemistry" and Encouraging Development Strategic Research Centers Program "Establishment of Consolidated Research Institute for Advanced Science and Medical Care" from the Ministry of Education, Culture, Sports, Science and Technology (MEXT), Japanese Government. The A3 Foresight Program "Synthesis and Structural Resolution of Novel Mesoporous Materials" supported by the Japan Society for Promotion of Science (JSPS) is also acknowledged.

Supporting information for this article is available on the WWW under http://www.angewandte.org or from the author.

deposited on linear resist moulds. The effect of the feature size W of the mold ($W = 0.1$–25 μm) on the final orientation of the mesochannels was studied by X-ray diffraction (XRD) and high-resolution scanning electron microscopy (HRSEM).

We determined beforehand the mesostructure of the P123-templated silica to be 2D hexagonal (*p6mm*) on the basis of HRSEM observations (see the Supporting Information). Bundles of cylindrical pores with a hexagonal arrangement were clearly observed. Our previous study also showed that a 2D hexagonal mesoporous silica film exhibited curved stripes on the top surface, and these stripes are not aligned along a uniaxial direction, that is, the orientation of the mesochannels on a flat substrate is random.[22]

Strictly aligned mesochannels with their long axes running parallel to both the substrate and the long axis of the mold were formed when the precursor was deposited on a mold with $W = 0.5$ μm. The geometry of the four-axis XRD is illustrated in the inset of Figure 2a. Out-of-plane (i.e., θ–2θ scan) and in-plane XRD (i.e., φ–$2\theta\chi$ and φ scans) were used to evaluate the arrangement of lattice planes parallel and normal, respectively, to the substrate. Here, the θ–2θ scanning profile showed two peaks at 1.1 and 2.1° ($d = 8.2$ and 4.2 nm, respectively; Figure 2a). The φ–$2\theta\chi$ scanning profile showed two peaks at 0.85 and 1.70° ($d = 10.4$ and 5.2 nm, respectively) when the incident X-rays were parallel to the long axis of the linear patterns (Figure 2b, trace A), whereas no peak was detected when the incident X-rays were perpendicular to the linear patterns (Figure 2b, trace B).

In general, the first peaks appearing in the θ–2θ and φ–$2\theta\chi$ scans are indexed as (10) and (11), respectively. However, we found that the arrangement of mesochannels here is different from that in previous reports.[17,18] In Figure 2e, one can clearly see multidomains of mesochannels in one linear pattern. A domain of hexagonally packed mesochannels formed from the substrate (bottom plane) is denoted the S-domain. The (10) plane of the mesochannels in the S-domain is parallel to the substrate. Another domain of mesochannels formed, from the resist (side plane), is denoted the R-domain, and the (10) plane of the mesochannels in the R-domain is perpendicular to the substrate. Hence, the two peaks in the θ–2θ scan are indexed as (11) and (22), and the two peaks in the φ–$2\theta\chi$ scan are indexed as (10) and (20) of the hexagonal structure in the R-domain. Although the hexagonal structure was slightly distorted, the d spacings of the peaks calculated from XRD patterns correspond well with those calculated from HRSEM images.

A scan of in-plane rotation φ of the sample was then conducted at a fixed detector position ($2\theta\chi = 0.85°$), and the periodic variation of the diffraction intensity was recorded. As shown in Figure 2c, two sharp peaks at ±90° (FWHM = 3.6°) demonstrate that the mesochannels are strictly aligned over the whole sample. This uniaxial orientation was further confirmed by HRSEM (Figure 2d and e). Multiple cross-sectional images of the patterns were taken, and all of them revealed a hexagonally packed arrangement of mesochannels (Figure 2e). Considering the thickness of the resist (0.5 μm), the feature size of the patterns (0.5 μm), and the pore-to-pore distance between mesochannels (ca. 10 nm), there are around 2000 mesochannels in one linear pattern.

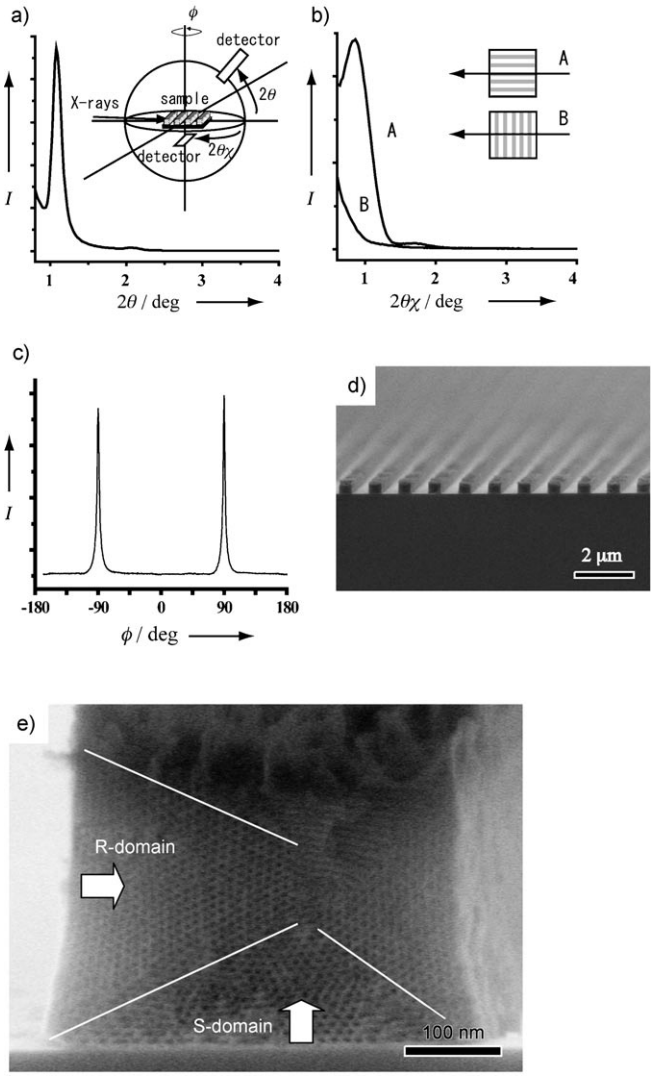

Figure 2. Two-dimensional hexagonal mesoporous silica patterns with $W = 0.5$ μm studied by XRD and HRSEM. a) Out-of-plane θ–2θ scan profile. Inset: illustration of the four axes of the goniometer used in the XRD measurements. b) In-plane φ–$2\theta\chi$ scan profile. The sample is set with the line patterns parallel (trace A) and perpendicular (trace B) to the incident X-rays. c) In-plane φ scan profile. Line patterns were set perpendicular to the incident X-rays at $\varphi = 0°$, and the detector was set at the position of the peak ($2\theta\chi = 0.85°$) detected in trace A of (b). d) Cross-sectional HRSEM images of the line patterns with a tilt angle of 10°. e) Enlarged HRSEM image for one of the line patterns showing uniaxially oriented mesochannels packed from the bottom plane (S-domain) and from the side plane (R-domain). The bumpy surface resulted from ICP treatment.

Because it is easy to spatially modulate patterns by lithography, we then attempted to control the orientation of the uniaxial mesochannels at designed locations. The silica precursor was deposited onto 0.5-μm linear molds with various patterns (Figure 3). In the case of a "–"-type pattern, the corresponding in-plane φ scanning profile (the arrow indicates the direction of $\varphi = 0°$) showed two peaks with a period of 180° (Figure 3a), which is usually observed in conventional uniaxially oriented mesoporous films.[17,18] Analogously, "+"- and "*"-type patterns showed peaks with

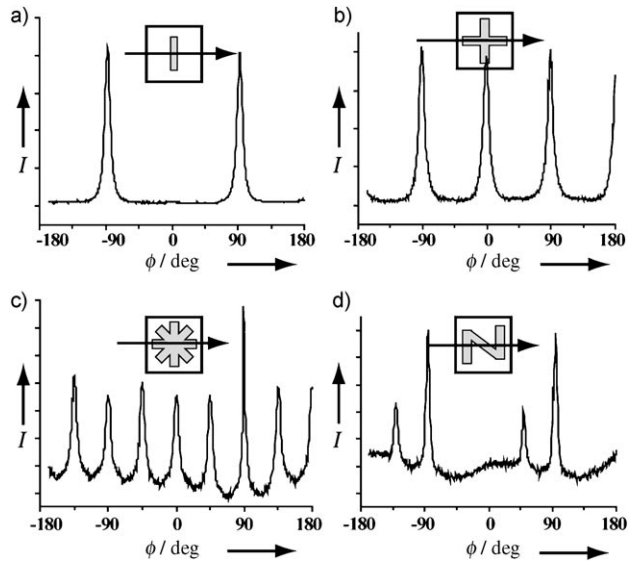

Figure 3. In-plane φ scanning profiles ($2\theta\chi$ set at 0.85°) of 0.5-μm mesoporous lines with various patterns (insets).

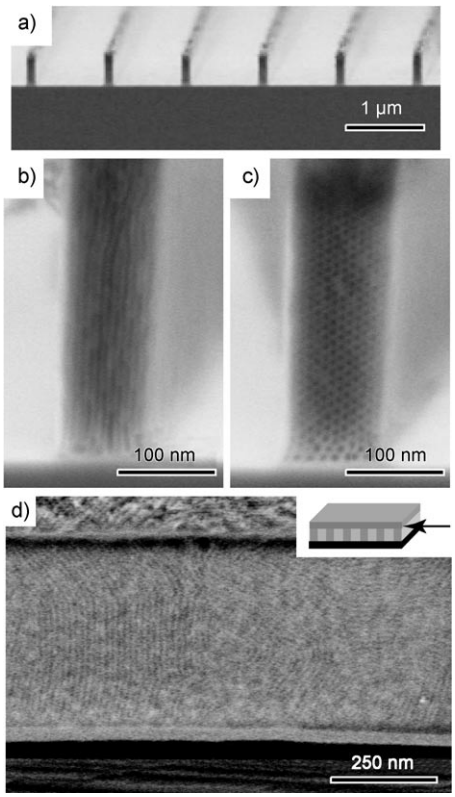

Figure 4. a–d) HRSEM images of mesoporous silica patterns with $W = 0.1$ μm. 2D hexagonal structure with the mesochannels running b) perpendicular or c) parallel to the substrate can be observed. d) View from the direction perpendicular to the line patterns (as indicated by the arrow in the inset) before removal of the resist.

periods of 90 and 45°, respectively (Figure 3b and c). However, the orientation at the intersectional positions was random (see the Supporting Information). In the case of a "Z"-type pattern, two peaks were obtained in both positive and negative φ regions. The distance between the peaks and the difference in peak intensities corresponded well to the designed angle and the area of the line patterns, respectively.

When the silica precursor was deposited onto 0.1-μm molds, cross-sectional HRSEM images showed that the mesochannels were aligned either perpendicular (Figure 4b) or parallel (Figure 4c) to the substrate. In the latter case, the mesochannels are packed almost exclusively from the side plane (only two or three layers of mesochannels are formed from the bottom plane), and the (10) plane of the mesochannels is perpendicular to the substrate. Another HRSEM image viewed from the direction perpendicular to the long axis of the linear patterns also revealed that the long axis of the mesochannels is oriented either perpendicular or parallel to the bottom plane, but all are parallel to the side plane (Figure 4d).

Previous studies have explained the mechanism of formation of mesostructures on a substrate in terms of an evaporation-induced self-assembly (EISA) process.[23,24] Mesostructures are generally formed from both the air/liquid interface (top plane) and the liquid/solid interface (bottom plane) during evaporation of solvents. Unlike a flat substrate, linear resist molds here provide a third interface, that is, the interface between liquid and resist (side plane), and several factors influence the interactions between the precursor and the side plane. These include interfacial hydrophobic interactions, shear stress, viscosity, and surface tension. We suggest that the final orientation of the mesochannel is mainly governed by the preferential alignment caused by bottom plane or side plane. In particular, the side plane plays a major role in regulating the orientation of mesochannels when the thickness of the resist (0.5 μm) is much larger than the feature size of the pattern (0.1 μm).

The evolution of the orientation of the mesochannels in confined linear nanospaces with decreasing feature size W is summarized in Figure 5. When W exceeds 0.5 μm (e.g., 1.0 μm), mesochannels are formed from the bottom plane. Both a hexagonally packed porous arrangement and an array of stripes can be observed, that is, these mesochannels are randomly oriented. The change in the in-plane φ scanning profiles indicates gradual development of uniaxial orientation with diminishing feature size (see the Supporting Information). In these cases, the large bottom plane induces parallel orientation of mesochannels, but uniaxial alignment is not achieved.

When W is about 0.5 μm, only the hexagonally packed porous arrangement appears. In this case, mesochannels are formed from both bottom (S-domain) and side (R-domain) planes (Figure 2 and Figure 5). We suggest that the mesochannels in the S- and R-domains stack simultaneously to form the final packing with a uniaxial orientation of mesochannels. By using this feature size, various types of uniaxially aligned mesoporous silicas can be fabricated (Figure 3). This is the first example of on-demand orientational control of cylindrical nanopores.

When W is less than 0.5 μm (e.g., 0.1 μm), the mesochannels are formed from the side plane, and this leads to a

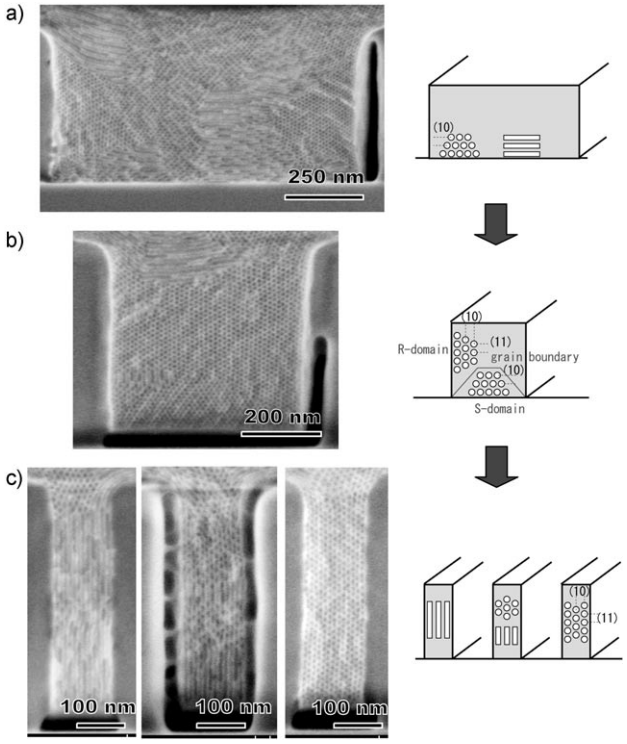

Figure 5. Cross-sectional HRSEM images and diagrams representing the orientation of the mesochannels in confined linear nanospaces with different feature sizes: a) >0.5 μm, b) ca. 0.5 μm, and c) <0.5 μm.

hexagonally packed porous arrangement or a stripe arrangement with the (10) plane perpendicular to the substrate. Orientation of the mesochannels is also observed for $W = 0.2$, 0.3, and 0.4 μm (see the Supporting Information). The stripe arrangement starts to appear when the feature size is less than 0.3 μm. In these cases, W is smaller than the thickness of the resist, so the influence of the side plane on the orientation becomes dominant. Although only a partially perpendicular orientation was obtained, a combination of nanospace confinement and an external field, such as a high magnetic field,[15] may be able to generate a fully perpendicular orientation.

In summary, we have presented a new approach for uniaxial alignment and orientational control of mesochannels from parallel to perpendicular to a substrate by coating a P123-templated silica solution onto lithographically prepared linear resist molds. Recently, Rice et al. fabricated metal nanowires by replication from mesoporous silica inside lithographically prepared silicon linear patterns.[26] They claimed that if one could further control the direction of aligned mesoporous channels and remove the excess film above the patterns, lithography-assisted alignment would be useful for electronic sensors and devices. Our process realizes such in-plane orientational control of the uniaxially aligned mesochannels, which is a significant step in the integration of bottom-up and top-down nanotechnologies for fabrication of advanced devices.

Experimental Section

Silicon substrates (n-type, ⟨100⟩, 4–6 Ω, 20×20 mm^2) were purchased from Shin-Etsu Chemical Co. and were cleaned in a H_2SO_4/H_2O_2 (1:1). An E.B. resist solution (ZEP520-A)[25] was purchased from Nippon Zeon Co. Tetraethoxysilane (TEOS) and triblock copolymer P123 were purchased from Sigma Aldrich and were used as inorganic silica source and structure-directing agent, respectively.

Resist films were initially prepared by spin coating the resist solution onto silicon substrates and then were baked on a hot plate at 180 °C for 3 min. The thickness of the resist was fixed at 0.5 μm. Linear resist molds with feature sizes (widths) of 0.1–25 μm and an area of 6×6 mm^2 (see the Supporting Information) were fabricated with an electron-beam lithography system (50 kV, ELS-7500EX, Elionix Co.). A P123-templated silica precursor solution was prepared by following our previous reports,[22] and the molar ratios of the precursor solution were TEOS/P123/EtOH/HCl/H_2O = 1:0.01:8.7:0.12:5.8. The precursor solution was spin coated (1000–8000 rpm) onto the resist molds. The direction of the mesoporous channels is fixed immediately after the formation of the 2D hexagonal structure through the EISA process. However, for further condensation of the silica framework, we aged as-coated samples in a constant atmosphere (ca. 23 °C, 46 % RH) for 2 d. After aging, the excess layers on the resist were removed by inductively coupled plasma (ICP) using C_3F_8. This process is necessary for the subsequent removal of the resist by O_2 plasma (see the Supporting Information). Finally, after calcination at 400 °C for 4 h to remove the surfactants, mesoporous silica patterns were generated.

Small-angle X-ray diffraction (SAXRD) patterns and in-plane XRD measurements were obtained with an X-ray diffractometer equipped with a four-axis goniometer (Rigaku ATX-G) using Cu_{K_α} radiation. The incident angle of X-rays was set to 0.2°.[18] High-resolution (HR) SEM and STEM images were taken with an SEM (Hitachi, S5500) without any metal coating.[22]

Received: February 14, 2007
Revised: April 13, 2007

Keywords: lithography · mesoporous materials · nanotechnology · self-assembly · template synthesis

[1] T. Yanagisawa, T. Shimizu, K. Kuroda, C. Kato, *Bull. Chem. Soc. Jpn.* **1990**, *63*, 988.
[2] C. T. Kresge, M. E. Leonowicz, W. J. Roth, J. C. Vartuli, J. S. Beck, *Nature* **1992**, *359*, 710.
[3] N. K. Mal, M. Fujiwara, Y. Tanaka, *Nature* **2003**, *421*, 350.
[4] C. H. Ko, R. Ryoo, *Chem. Commun.* **1996**, 2467.
[5] P. Yang, G. Wirnsberger, H. C. Huang, S. R. Cordero, M. D. McGehee, B. Scott, T. Deng, G. M. Whitesides, B. F. Chmelka, S. K. Buratto, G. D. Stucky, *Science* **2000**, *287*, 465.
[6] A. Fukuoka, H. Miyata, K. Kuroda, *Chem. Commun.* **2003**, 284.
[7] W. C. Molenkamp, M. Watanabe, H. Miyata, S. H. Tolbert, *J. Am. Chem. Soc.* **2004**, *126*, 4476.
[8] R. Fan, R. Karnik, M. Yue, D. Y. Li, A. Majumdar, P. D. Yang, *Nano Lett.* **2005**, *5*, 1633.
[9] G. Wirnsberger, B. J. Scott, G. D. Stucky, *Chem. Commun.* **2001**, 119.
[10] C. M. Yang, A. T. Cho, F. M. Pan, T. G. Tsai, K. J. Chao, *Adv. Mater.* **2001**, *13*, 1099.
[11] H. M. Luo, D. H. Wang, J. B. He, Y. F. Lu, *J. Phys. Chem. B* **2005**, *109*, 1919.
[12] H. W. Hillhouse, J. W. van Egmond, M. Tsapatsis, *Langmuir* **1999**, *15*, 4544.
[13] N. A. Melosh, P. Davidson, P. Feng, D. J. Pine, B. F. Chmelka, *J. Am. Chem. Soc.* **2001**, *123*, 1240.

[14] S. H. Tolbert, A. Firouzi, G. D. Stucky, B. F. Chmelka, *Science* **1997**, *278*, 264.
[15] Y. Yamauchi, M. Sawada, T. Noma, H. Ito, S. Furumi, Y. Sakka, K. Kuroda, *J. Mater. Chem.* **2005**, *15*, 1137.
[16] M. Trau, N. Yao, E. Kim, Y. Xia, G. M. Whitesides, I. A. Aksay, *Nature* **1997**, *390*, 674.
[17] H. Fukumoto, S. Nagano, N. Kawatsuki, T. Seki, *Adv. Mater.* **2005**, *17*, 1035.
[18] H. Miyata, K. Kuroda, *Chem. Mater.* **1999**, *11*, 1609.
[19] B. C. Chen, H. P. Lin, M. C. Chao, C. Y. Mou, C. Y. Tang, *Adv. Mater.* **2004**, *16*, 1657.
[20] P. D. Yang, T. Deng, D. Y. Zhao, P. Y. Feng, D. Pine, B. F. Chmelka, G. M. Whitesides, G. D. Stucky, *Science* **1998**, *282*, 2244.
[21] C.-W. Wu, T. Aoki, M. Kuwabara, *Nanotechnology* **2004**, *15*, 1886.
[22] C.-W. Wu, Y. Yamauchi, T. Ohsuna, K. Kuroda, *J. Mater. Chem.* **2006**, *16*, 3091.
[23] Y. F. Lu, R. Ganguli, C. A. Drewien, M. T. Anderson, C. J. Brinker, W. L. Gong, Y. X. Guo, H. Soyez, B. Dunn, M. H. Huang, J. I. Zink, *Nature* **1997**, *389*, 364.
[24] D. Grosso, F. Cagnol, G. Soler-Illia, E. L. Crepaldi, H. Amenitsch, A. Brunet-Bruneau, A. Bourgeois, C. Sanchez, *Adv. Funct. Mater.* **2004**, *14*, 309.
[25] B. S. Kim, H. S. Lee, J. S. Wi, K. B. Jin, K. B. Kim, *Jpn. J. Appl. Phys.* **2004**, *44*, L95.
[26] R. L. Rice, D. C. Arnold, M. T. Shaw, D. Iacopina, A. J. Quinn, H. Amenitsch, J. D. Holmes, M. A. Morris, *Adv. Funct. Mater.* **2007**, *17*, 133.

